Nonlinear Dynamics **24:** 333–358, 2001.

On the Dynamics of a Harmonic Oscillator Undergoing Impacts with a Vibrating Platform

S. SALAPAKA, M. DAHLEH, and I. MEZIĆ
Department of Mechanical and Environmental Engineering, University of California, Santa Barbara, CA 93106, U.S.A.

(Received: 16 July 1999; accepted: 22 August 2000)

Abstract. This paper deals with a model for repeated impacts of a mass attached to a spring with a massive, sinusoidally vibrating table. This model has been studied in an attempt to understand the cantilever-sample dynamics in atomic force microscopy. In this work, we have shown that for some values of the frequency of the vibrating table, there are countably many orbits of arbitrarily long periods and the system is sensitive to the initial conditions with which the experiments are conducted. We have also shown existence of complex dynamics in the cases when the natural frequency of the spring-mass system is very low; and when it is the same as the oscillating frequency of the table.

Keywords: Impact oscillators, AFMs, bifurcations, complex dynamics, resonance, soft springs, Hausdorff dimension, symbolic dynamics, sensitive dependence on initial conditions.

1. Introduction

In recent years, many repeated-impact dynamical systems have been studied. The model for repeated impacts of a ball with a massive, sinusoidally vibrating table is extensively studied in [1, pp. 104–116].

A periodically forced oscillator with harmonic excitation with a wall that restricts its motion to one side of the equilibrium position is discussed in [2]. The behaviour of an impact oscillator with an offset, (i.e. the position of the wall is not at the rest point of the oscillator) is given in [3]. Nordmark [4] and Chin et al. [5] deal with new types of bifurcations (*grazing bifurcations*) that arise in systems which evolve from a nonimpacting to an impacting state (or vice versa) as a system parameter varies smoothly. In this paper, we consider a spring-mass system and a massive table vibrating below it such that the rest positions of the table and the mass are not the same. This system models an experiment that we conducted using an Atomic Force Microscope (AFM). The description of the device and the experiment is given in Section 7. We observed the appearance of subharmonics as the amplitude of the vibration of the piezoelectric tube was increased, which suggested the existence of complex dynamics. This stimulated our interest to develop a model to explore these dynamics. A similar model has been considered by Berg and Briggs [6] who are also motivated by similar experiments in atomic force microscopy. They have studied the regions in parameter space that guarantee the stability of single-impact periodic orbits. In our paper, the model is used not only to study these stability regions but also to show the existence of complex dynamics. In fact, we prove that our model is equivalent to the well known chaotic *Bernoulli shift map* [7] for certain parameter values and furthermore show the existence of a *horseshoe* [8] in it. Also, we have analyzed the dependence of the dynamics of the model on the natural frequency, ω_n, of the

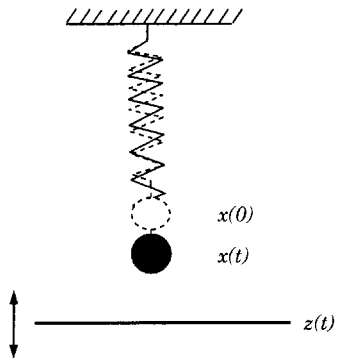

Figure 1. The model for cantilever-sample system.

spring. We found out that *the bouncingball system* described in [1] comes as a limiting case ($\omega_n = 0$) of this study. Our analysis reproduces all the results in [1]. We have shown that some of the assumptions that were made in [1] for mathematical simplicity were not necessary to obtain the results.

In Section 2, we have described the model of the repeated impact oscillator. In Section 3, a detailed study of the system for a specific set of system parameters (the ratio of the natural frequency to the table frequency; and the amplitude of vibration of the table), is presented. In Section 4, we study how the single impact periodic orbits change as we vary the system parameters. In Section 5, the period doubling bifurcations have been shown to exist when the system has very low (tending to zero) natural frequencies. In Section 6 similar results have been presented when the natural frequency of the spring-mass system matches that of the frequency of oscillation of the table. The experiment that we conducted which motivated this study is presented in Section 7. Some observations and conclusions have been outlined in Section 8.

2. Model Description

We consider a spring-mass system with natural frequency ω_n, and a massive table vibrating below it such that the rest positions of the table and the mass are not the same. Figure 1 shows the visualization of the system. Here all variables are measured from the equilibrium position of the mass and the upward direction is considered as positive. The rest position of the mass is at $x = 0$ and the position of the table is described by the equation $z(t) = -p + \beta \sin(\omega t)$. It is assumed that the mass of the table is large and therefore its motion is not altered by the impacts between the mass and the table. The equation governing the motion of the mass under no external forcing is given by

$$\ddot{x} + {\omega_n}^2 x = 0. \tag{1}$$

The solution to this differential equation with initial displacement x_o and initial velocity $\dot{x}_o$ (at $t = t_0$) is given by

$$x(t) = x_o \cos(\omega_n(t - t_0)) + \frac{\dot{x}_o}{w_n} \sin(\omega_n(t - t_0)), \tag{2}$$

$$\dot{x}(t) = \dot{x}_o \cos(\omega_n(t - t_0)) - \omega_n x_o \sin(\omega_n(t - t_0)). \tag{3}$$

The dissipation of energy by the mass in an impact is captured by the coefficient of restitution ε. To study this model, we have to solve the differential equation (1) repeatedly with initial conditions being redefined at every impact. If we denote the sequence of time instants at which the impacts take place by $\{t_k\}$, $k \in \mathbb{N}$, and the speed of the mass just before the impact at time instant t_k by v_k, then the motion of the mass in the time interval $(t_k, t_{k+1}]$ is given by Equations (2) and (3), where the initial conditions are given by

$$x_o = -p + \beta \sin(\omega t_k), \tag{4}$$

$$\dot{x}_o = -\varepsilon v_k + (1+\varepsilon)\beta\omega \cos(\omega t_k). \tag{5}$$

These equations hold for the impacts after which the mass and the table separate (that is, $x(t) - z(t) > 0$ for all $t \in (t_k, t_{k+1})$). The initial condition $\dot{x_o}$ (which is the velocity of mass just after impact) is obtained from the definition of coefficient of restitution. It is defined as the negative of the ratio between the relative velocities after and before impact, i.e.

$$\varepsilon = -\frac{\dot{x_o} - \beta\omega\cos(\omega t)}{v_k - \beta\omega\cos(\omega t)}.$$

We know that at the instant t_{k+1}, the following relations hold

$$x(t_{k+1}) - z(t_{k+1}) = 0, \tag{6}$$

$$v_{k+1} = \dot{x}(t_{k+1}), \tag{7}$$

where the initial conditions are given by (4) and (5). After substituting (4), (5), (2) and (3) in (6) and (7), we obtain the following equations

$$(-p + \beta \sin(\omega t_k)) \cos(\omega_n \Delta_k^t) + \frac{-\varepsilon v_k + (1+\varepsilon)\beta\omega\cos(\omega t_k)}{\omega_n} \sin(\omega_n \Delta_k^t) + p - \beta \sin(\omega t_{k+1}) = 0, \tag{8}$$

$$v_{k+1} = (\omega_n p - \beta\omega_n \sin(\omega t_k)) \sin(\omega_n \Delta_k^t) + ((\varepsilon+1)\beta\omega\cos(\omega t_k) - \varepsilon v_k)\cos(\omega_n \Delta_k^t), \tag{9}$$

where $\Delta_k^t = t_{k+1} - t_k$. In fact, we will use this notation from now onwards in this report. That is, by Δ_a^k, we will denote $a_{k+1} - a_k$. Note that the above equations are transcendental and therefore cannot be solved in a closed form. We also see that, in the case of plastic impacts (i.e. $\varepsilon = 0$), Equation (8) becomes independent of the speed v_k. Physically, this corresponds to the impacts in which there is no rebound. In this case the knowledge of the position of the table at impact completely determines the motion of the mass and therefore we do not need to know the velocity of the mass just before impact. Even though the impacts are plastic, the mass and the table eventually separate because of the restoring force of the spring and the vibration of the table. We nondimensionalize Equation (8) by introducing the variables: scaled impact time $\psi_k = \omega t_k$, the amplitude $\nu = -\beta/p$ and the frequency ratio $\eta = \omega_n/\omega$. This results in the following equation for the plastic case (i.e. $\varepsilon = 0$),

$$(1 + \nu \sin(\psi_k)) \cos(\eta \Delta_k^\psi) + \frac{\nu}{\eta} \cos(\psi_k) \sin(\eta \Delta_k^\psi) - 1 - \nu \sin(\psi_{k+1}) = 0. \tag{10}$$

Related to the scaled impact time, we introduce a phase variable, $\phi := \psi \bmod 2\pi$. This variable represents the position of the table at time instant ϕ. We know that, when the impacts are

plastic, given an impact phase, the next phase at which impact occurs is uniquely determined. We denote this mapping by $f_{\eta,\nu}$: $\phi_i \to \phi_{i+1}$, $\phi \in [0, 2\pi)$.

As we have already mentioned, the equations above are true for those impacts, immediately after which, the mass and the table separate. Now, we shall consider the impacts after which, the mass and the table stick to each other till they eventually separate. The sticking happens when the relative velocity, $\dot{x}(t)-\dot{z}(t)$, is negative at the instant of impact. The negative velocity at the instant of impact implies that the mass would have gone below the table, which is physically impossible. So, the mass sticks to the plate till the restoring forces on the mass (due to the spring) just overcomes the 'pushing' force on it (due to the vibrating plate). Note that, after these impacts, the mass moves with the same velocity and acceleration as the table. Also, the motion of the table is not altered by these impacts because of its infinite mass. At separation, the acceleration of the mass is equal to that of the plate, and the following relation holds,

$$\ddot{z}_s = -\omega_n^2 z_s,$$

where z_s is the position at which the mass and the plate separate. So we have

$$-\beta\omega^2 \sin(\omega t_s) = -\omega_n^2(-p + \beta \sin(\omega t_s)),$$

where t_s is the time instant of separation. Substituting $\phi_s = \omega t_s \bmod 2\pi$, the phase at separation, and nondimensionalizing the above equation, we obtain

$$-\frac{\nu}{\eta^2}\sin(\phi_s) = -1 - \nu \sin(\phi_s).$$

This equation can be simplified as

$$\sin(\phi_s) = \frac{\eta^2}{\nu(1-\eta^2)}.$$

Using this phase value (ϕ_s) and Equation (10), we can compute the next impact phase (see the Appendix for the details). Thus we can extend the definition of the mapping $f_{\eta,\nu}$ for those impacts, immediately after which, the mass and the table do not separate.

3. Sensitive Dependence on Initial Conditions: Inelastic Impacts

In this section, it will be shown that the map $f_{\eta,\nu} : \phi_i \to \phi_{i+1}$ is sensitive to initial conditions for certain parameter values. Note that this map cannot be obtained analytically as equation (10) is transcendental. However, this function can be constructed by numerical means for a given value of η and over a discrete set of values of phase, $\phi \in [0, 2\pi]$.

In Figure 2, we show the plot $f_{\eta,\nu}$ *versus* ϕ with $(\eta, \nu) = (0.2121, -0.2)$ and $\phi \in I := [1.11, 1.32]$. Note that the interval has been partitioned into three smaller intervals and I_0 and I_1 are closed intervals. Let Λ be the set of all those points in I that are not mapped out of I by repeated application of $f_{\eta,\nu}$ on them. That is,

$$\begin{aligned}\Lambda &= \{\phi \in I : f_{\eta,\nu}^n(\phi) \in I \text{ for all } n \in \mathbb{N}\} \\ &= \bigcap_{n=0}^{\infty} f_{\eta,\nu}^{-n}(I).\end{aligned}$$

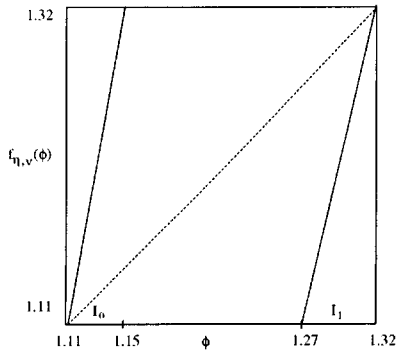

Figure 2. The map $f_{\eta,\nu}$ for $\eta = 0.2121$ and $\nu = -0.2$. $f_{\eta,\nu}(\phi)$ for ϕ in [1.15, 1.27] is not in [1.11, 1.32] and not shown in this figure.

Note that, if $\phi \in \Lambda$, then ϕ has to be in $I_0 \cup I_1$, because if $\phi \notin I_0 \cup I_1$ then $f_{\eta,\nu}(\phi) \notin I$ (see Figure 2). To every point, ϕ_0 in Λ we can associate a sequence $\{\alpha_k\}$, $k \in \mathbb{N}$ such that

$$\alpha_k = 0 \quad \text{if} \quad f^k_{\eta,\nu}(\phi_0) \in I_0,$$

$$\alpha_k = 1 \quad \text{if} \quad f^k_{\eta,\nu}(\phi_0) \in I_1.$$

This is always possible since otherwise $f^{k+1}_{\eta,\nu}(\phi_0) \notin I$. We define a space of infinite sequences, Σ by

$$\Sigma = \{0.x_1x_2 \ldots . \text{ such that } x_i \in \{0, 1\} \text{ for all } i \in \mathbb{N}\}.$$

We also define a map $h : \Lambda \to \Sigma$ by $h(\phi_0) = 0.\alpha_1\alpha_2\alpha_3 \ldots$, where $\alpha_k, k \in \mathbb{N}$ are obtained as described above. We have introduced these sequences into this analysis because it can be shown that the space of these sequences is homeomorphic to the invariant set Λ. Thus we can find the properties of the underlying set Λ by studying Σ. In the next section, we will study this sequence space.

3.1. Symbolic Dynamics

A good reference of this material can be found in [8]. We define a metric $d(,\cdot,)$ on Σ by $d(x, y) = \sum_{i=1}^{\infty} \frac{|x_i - y_i|}{2^i}$, where $x = 0.x_1x_2x_3\ldots$, $y = 0.y_1y_2y_3\ldots$. Let $s^i, i \in \mathbb{N}$ denote all finite binary sequences of i bits. Note that for every $i \in \mathbb{N}$ there exist 2^i i-bit sequences. Let us denote these by $s^i_1, s^i_2, \ldots s^i_{2^i}$. We also define the shift map $\sigma : \Sigma \to \Sigma$ by $\sigma(0.x_1x_2x_3\ldots) = 0.x_2x_3x_4\ldots$.

The sequence of binary sequences generated by repeated application of the map σ to a point in Σ is called an *orbit* of σ. An orbit of σ is *i-periodic* (or has *period i*) if $\sigma^i(x) = x$ for all x in the orbit. Now, we state three facts concerning the dynamics of σ on Σ in the following theorem.

THEOREM 1. *The shift map σ has*

1. *countably many periodic orbits of arbitrarily high periods;*
2. *uncountably many nonperiodic orbits;*
3. *a dense orbit.*

Proof. See [8, pp. 430–438] for the proof. □

From Figure 2, we note that $\gamma_1 := 5.25 \geq \partial f_{\eta,\nu}/\partial\phi \geq \gamma_2 := 4.2$ for all $\phi \in \text{int}(I_0) := (c_0, d_0) = (1.11, 1.15)$ and for all $\phi \in \text{int}(I_1) := (c_1, d_1) = (1.27, 1.32)$. Also note the function $f_{\eta,\nu}$ is monotonically increasing on I_0 and I_1 and therefore $f_{\eta,\nu}^{-1}(J)$ consists of two closed intervals, one in I_0 and another in I_1, where J is any closed interval in I_0 or I_1. Also, the length of each of these intervals is less than $(1/\gamma_2)|J|$ where $|J|$ represents the usual length of the interval.

THEOREM 2. *The map $h : \Lambda \to \Sigma$ is a homeomorphism.*

Proof. We need only to show that h is one-one, onto and continuous since the continuity of the inverse of h will follow from the fact that one-one, onto and continuous maps from compact sets into Hausdorff spaces are homeomorphisms [8, p. 434].

Let $I_{\alpha_1\alpha_2\ldots\alpha_n}$ denote the set, $I_{\alpha_1} \cap f_{\eta,\nu}^{-1}(I_{\alpha_2}) \cap f_{\eta,\nu}^{-2}(I_{\alpha_3}) \ldots \cap f_{\eta,\nu}^{-n+1}(I_{\alpha_n}) = I_{\alpha_1} \cap f_{\eta,\nu}^{-1}(I_{\alpha_2} \cap f_{\eta,\nu}^{-1}(I_{\alpha_3} \ldots \cap f_{\eta,\nu}^{-1}(I_{\alpha_n}) \ldots))$ where $\alpha_i \in \{0, 1\}$. Note that for every point ϕ in $I_{\alpha_1\alpha_2\ldots\alpha_n}$, $h(\phi) = .\beta_1\beta_2\ldots$ is such that $\beta_i = \alpha_i, i \in \{1, 2 \ldots n\}$. As $f_{\eta,\nu}^{-1}(I_{\alpha_k}) \cap I_j$ is a closed interval for all $k \in \mathbb{N}$, $j \in \{0, 1\}$, $I_{\alpha_1\alpha_2\ldots\alpha_n}$ is a closed interval. From the definition of $I_{\alpha_1\alpha_2\ldots\alpha_n}$, it follows that $I_{\alpha_1\alpha_2\ldots\alpha_{n+1}} \subset I_{\alpha_1\alpha_2\ldots\alpha_n}$. As the slope of $f_{\eta,\nu} > \gamma_2$ at all points in I_j, $j \in \{0, 1\}$, $|I_{\alpha_1\alpha_2\ldots\alpha_{n+1}}| < (1/\gamma_2)|I_{\alpha_1\alpha_2\ldots\alpha_n}|$.

h is one-one: This means that given $\phi, \phi' \in \Lambda$, if $\phi \neq \phi'$, then $h(\phi) \neq h(\phi')$. Let us prove by contradiction, suppose $\phi \neq \phi'$ and

$$h(\phi) = h(\phi') = .x_1x_2\ldots x_n\ldots;$$

then by construction of Λ we know that $\phi \in I_{x_1x_2\ldots x_n}$ and $\phi' \in I_{x_1x_2\ldots x_n}$ for all $n \in \mathbb{N}$. But, $\{I_{x_1x_2\ldots x_n}\}$ is a nested sequence of closed bounded intervals whose lengths shrink to zero, therefore by a theorem due to Cantor (see theorem 1.2 in [9]), $\cap_{n=1}^{\infty} I_{x_1x_2\ldots x_n}$ contains a unique point, and hence $\phi = \phi'$. However, this contradicts our supposition that $\phi \neq \phi'$. This shows h is $one - one$.

h is onto: Let $y = .y_1y_2\ldots \in \Sigma$ be arbitrarily chosen. By Cantor's theorem, we know that $\cap_{n=1}^{\infty} I_{y_1y_2\ldots y_n}$ is a unique point in Λ. Let this point be denoted by ϕ_1. Then by construction of Λ and definition of h we have $y = h(\phi_1)$. As y was chosen arbitrarily in Σ, we have shown that h is an $onto$ function.

h is continuous: This means that given any point $\psi \in \Lambda$ and $\varepsilon > 0$, we can find a $\delta > 0$ such that $|\psi' - \psi| < \delta$ implies $d(h(\psi'), h(\psi)) < \varepsilon$. Let $\varepsilon > 0$ and $\psi \in \Lambda$ with $h(\psi) = 0.\psi_1\psi_2\ldots$ be given. From the definition of the metric on Σ, we know that there exists $N = N(\varepsilon)$ in $\mathbb{N}$ such that for any $z = 0.z_1z_2\ldots \in \Sigma$ with $z_i = \psi_i, i \in \{1, 2 \ldots N\}$, $d(h(\psi), z) < \varepsilon$. We know that for each θ in Λ such that $|\psi - \theta| < \delta := 1/\gamma_1^N|I|$, $h(\theta)$ has the form $0.\psi_1\psi_2\ldots\psi_N\theta_{N+1}\theta_{N+2}$ where $\theta_i \in \{0, 1\}$. This in turn implies that $d(h(\psi), h(\theta)) < \varepsilon$. Thus h is continuous. □

Now, we can state a theorem regarding the dynamics of $f_{\eta,\nu}$ on Λ that is precisely the same as theorem (1), which describes the dynamics of σ on Σ. The sequence of points generated by repeated application of the map $f_{\eta,\nu}$ to a point in Λ is called an $orbit$ of $f_{\eta,\nu}$. An orbit of $f_{\eta,\nu}$ is $i\text{-}periodic$ (or has $period\ i$) if i is the least positive integer such that $f_{\eta,\nu}^i(x) = x$ for all x in the orbit. We say that an orbit $\mathcal{O}$ is *eventually i periodic* if there exists a finite number M in $\mathbb{N}$ such that the sequence in Λ obtained by calculating $\{f_{\eta,\nu}^M(x)\}$ for every $x \in \mathcal{O}$

forms an i periodic orbit. Any orbit that is neither periodic nor eventually periodic is said to be *nonperiodic*.

THEOREM 3. *The map $f_{\eta,\nu}$ has*

1. *countably many periodic orbits of arbitrarily high periods;*
2. *uncountably many nonperiodic orbits;*
3. *a dense orbit.*

Proof. First, we show that $f_{\eta,\nu}$ acting on Λ and σ acting on Σ are topological conjugates, i.e. $h \circ f_{\eta,\nu}(\phi) = \sigma \circ h(\phi)$ for all $\phi \in \Lambda$. Let $\phi \in \Lambda$. Therefore, there exists a binary sequence, $\{\alpha_k\}$ such that $\phi = \bigcap_{n=1}^{\infty} I_{\alpha_1\alpha_2\ldots\alpha_n}$. Therefore $f_{\eta,\nu}(\phi) = \bigcap_{n=2}^{\infty} I_{\alpha_2\alpha_3\ldots\alpha_n}$. From the definition of σ, we have $h(f_{\eta,\nu}(\phi)) = .\alpha_2\alpha_3\ldots$ and $\sigma(h(\phi)) = \sigma(.\alpha_1\alpha_2\ldots) = (.\alpha_2\alpha_3\ldots)$. This shows that $h \circ f_{\eta,\nu}(\phi) = \sigma \circ h(\phi)$.

The theorem is an immediate consequence of topological conjugacy of f acting on Λ with σ acting on Σ and Theorems 1 and 2. □

3.2. Hausdorff Dimension of the Invariant Set Λ

In this section we will find the Hausdorff dimension (see the Appendix for the definition) of the invariant set Λ. A good exposition on this dimension is given in [9].

Here, we are making simplifying assumptions that $f_{\eta,\nu}(\phi)$ varies linearly with ϕ on the intervals I_0 and I_1. This approximate figure has been shown in Figure 3a. The slopes of these lines are $\lambda_0 = 5.25$ and $\lambda_1 = 4.2$ respectively. Now, this invariant set was defined by

$$\begin{aligned}\Lambda &= \{\phi \in I : f^n_{\eta,\nu}(\phi) \in I \text{ for all } n \in \mathbb{N}\}\\ &= \bigcap_{n=0}^{\infty} f^{-n}_{\eta,\nu}(I).\end{aligned}$$

Let us construct this set graphically. Figure 3 shows how we obtain $f^{-1}_{\eta,\nu}(I)$ and $f^{-2}_{\eta,\nu}(I)$. Note that, $f^{-1}_{\eta,\nu}(I)$ consists of two closed intervals I_0 and I_1; $f^{-2}_{\eta,\nu}(I)$ consists of four closed intervals I_{00}, I_{01}, I_{10} and I_{11}. Also, note that $|I_{ij}| = \eta_i\eta_j|I|$; $i, j \in \{0, 1\}$, where $\eta_i = 1/\lambda_i$. If we proceed in this manner we observe that

1. $f^{-n}_{\eta,\nu}(I)$ consists of 2^n closed intervals in $\mathcal{F}_n := \{I_{0\ldots0}, I_{0\ldots01}, \ldots, I_{1\ldots1}\}$;
2. $\Lambda \subset E_n := I_{0\ldots0} \cup I_{0\ldots01} \cup \ldots \cup I_{1\ldots1}$;
3. $|I_{\alpha_1\ldots\alpha_n}| = \eta_{\alpha_1}\eta_{\alpha_2}\ldots\eta_{\alpha_n}|I|$.
4. $|I_{0\ldots0}|^s + |I_{0\ldots01}|^s + \ldots + |I_{1\ldots1}|^s = (\eta_0^s + \eta_1^s)^n|I|^s$ for all $s > 0$;

Now, we shall show that Λ is a Cantor set. In the following theorems we shall use these observations and notation.

THEOREM 4. *Λ is a Cantor set.*

Proof. We note that for each $n \in \mathbb{N}$, E_n is union of finite number of closed intervals. Therefore, E_n is a closed bounded set for every $n \in \mathbb{N}$. Also, $\Lambda = \bigcap_{n=0}^{\infty} E_n$, is an infinite intersection of closed sets. Hence Λ is a closed bounded set in $\mathbb{R}$ (i.e. a compact set). From

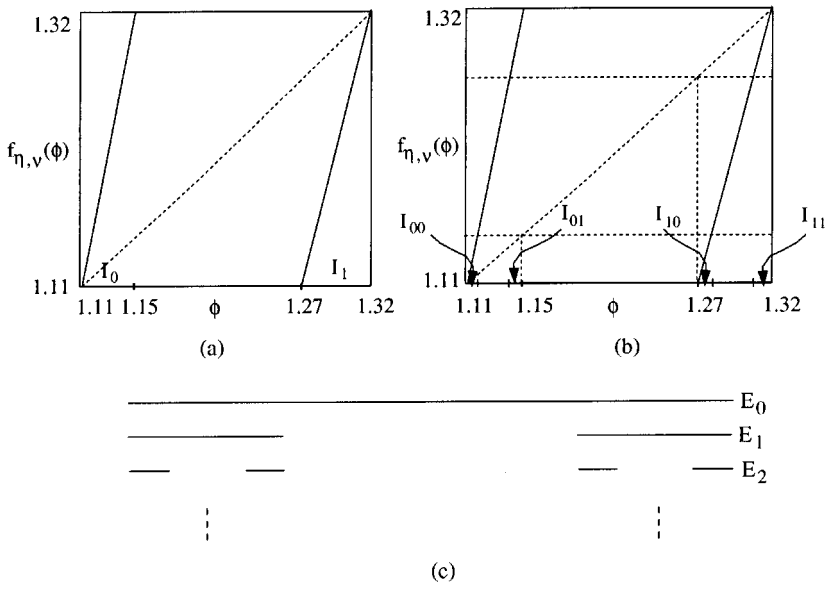

Figure 3. (a), (b) The construction of set Λ. (c) The Cantor set.

the graphical construction of the set Λ we see that it is nowhere dense and that every neighbourhood of every point of Λ has at least another point of Λ. This shows that Λ is a perfect set.

So, we see that Λ is a nonempty, compact, nowhere dense and perfect set. This implies that Λ is a Cantor set. □

Now, we shall calculate the Hausdorff dimension of the set Λ. Let $s_o > 0$ be such that $\eta_0^{s_o} + \eta_1^{s_o} = 1$. Now, $\eta_0 = 0.1905$ and $\eta_1 = 0.2381$, and s_o evaluates to $0.449\ldots$.

CLAIM 1. *The Hausdorff dimension of the set* Λ *is* s_o.

This proof uses concepts from the measure theory (see the Appendix for these concepts).

Proof. First, we show that $\mu_n^{*(s_o)}(\Lambda) \leq |I|^{s_o}$ for some $n \in \mathbb{N}$. Now, $\mu_n^{*(s_o)}(\Lambda)$ is the outer measure obtained from the covering family $\mathcal{T}_n$ and the premeasure τ where

$$\mathcal{T}_n \quad \{T : T \text{ is an open interval and diameter}(T) \leq \eta_1^n |I|\}$$

$$\text{and } \tau(T) = (\text{diameter}(T))^{s_o},\ T \in \mathcal{T}_n.$$

Let L_j, $j \in \{1, 2, 3 \ldots 2^{n+1}\}$ be the 2^{n+1} closed intervals corresponding to $f_{\eta,\nu}^{-(n+1)}(I)$. Note that $|L_j| \leq \eta_1^{n+1}|I|$ for all $j \in \{1, 2 \ldots 2^{n+1}\}$. Let $0 < \varepsilon < \eta_1^n - \eta_1^{n+1}$, and let L'_j, $j \in \{1, 2 \ldots 2^{n+1}\}$ be 2^{n+1} open intervals such that $L_j \subset L'_j$ and $||L_j| - |L'_j|| \leq \varepsilon/2^{n+1}$. This implies that L'_j is in $\mathcal{T}_n$ for all j. Now

$$\mu_n^{*(s_o)}(\Lambda) = \inf \left\{ \sum_{k=1}^{\infty} \tau(T_k) : T_k \in \mathcal{T}_n \text{ and } \Lambda \subset \cup_{k=1}^{\infty} T_k \right\}$$

and therefore

$$\mu_n^{*(s_o)}(\Lambda) \ \leq \ \sum_{k=1}^{2^{n+1}} \tau(L'_k) \leq \sum_{k=1}^{2^{n+1}} \left(\tau(L_k) + \frac{\varepsilon}{2^{n+1}} \right)$$

$$\leq (\eta_0^{s_o} + \eta_1^{s_o})^{n+1}|I|^{s_o} + \varepsilon = |I|^{s_o} + \varepsilon. \tag{11}$$

As ε was chosen arbitrarily, we have

$$\mu_n^{*(s_o)}(\Lambda) \leq |I|^{s_o}. \tag{12}$$

Now, we shall show that $\mu_n^{*(s_o)}(\Lambda) \geq |I|^{s_o}$. Let $\mathcal{J}$ be any collection of open intervals G_i, $i \in \mathbb{N}$ containing Λ. We make the following observations.

1. As Λ is a compact set, there exists a finite subcover of Λ, $\mathcal{J}_p = \{G_{\alpha_k}\}, k \in \{1, \ldots, p\}$.
2. Every open interval $J \subset I$ with $J \cap \Lambda \neq \phi$, contains some pair of closed intervals, that occur in the graphical construction of the set Λ. If we call largest such intervals as H_0 and H_1, then J contains H_0 followed by an open interval K in compliment of Λ, followed by H_1.

Let $J \in \mathcal{J}_p$. If $J \cap \Lambda \neq \phi$, then let H_0, K, and H_1 be the corresponding intervals as discussed above. If $J \cap \Lambda = \phi$, then let $H_0 = \phi$, $H_1 = \phi$ and $K = J$. Without loss of generality, let $|H_0| \geq |H_1|$, and note that, from the construction of the Cantor set we have

1. $|K| \geq \dfrac{1 - \eta_0 - \eta_1}{\eta_0}|H_0|$.
2. $|H_1| \leq \dfrac{\eta_1}{\eta_0}|H_0|$.
3. The function
   $$q(x) := \left(\frac{1 - \eta_1}{\eta_0} + x\right)^{s_o} - 1 - x^{s_o}$$
   is a monotonically decreasing function and therefore
   $$q(x) > q(\frac{\eta_1}{\eta_0}) = 0 \quad \text{for all } x < \frac{\eta_1}{\eta_0}.$$

So we have

$$|J|^{s_o} \geq (|H_0| + |K| + |H_1|)^{s_o} \geq \left(|H_0| + \frac{1 - \eta_0 - \eta_1}{\eta_0}|H_0| + |H_1|\right)^{s_o}$$
$$= \left(\frac{1 - \eta_1}{\eta_0}|H_0| + |H_1|\right)^{s_o},$$

that is

$$|J|^{s_o} \geq \left(\frac{1 - \eta_1}{\eta_0} + \frac{|H_1|}{|H_0|}\right)^{s_o}|H_0|^{s_o} \geq \left(1 + \left(\frac{|H_1|}{|H_0|}\right)^{s_o}\right)|H_0|^{s_o} = |H_0|^{s_o} + |H_1|^{s_o}.$$

Thus replacing every such J by the two subintervals H_0 and H_1 does not increase the sum $\sum_{J \in \mathcal{J}_p} |J|^{s_o}$. We proceed in this way until, after a finite number of steps, we reach a covering of Λ by intervals in $\mathcal{F}_m$ (i.e. intervals corresponding to $f_{\eta,\nu}^{-m}(I)$). So, we have shown that there exists an $m \in \mathbb{N}$ such that

$$\sum_{J \in \mathcal{J}} |J|^{s_o} \geq \sum_{J \in \mathcal{J}_p} |J|^{s_o} \geq \sum_{J \in \mathcal{F}_m} |J|^{s_o}$$
$$= (\eta_0^{s_o} + \eta_1^{s_o})^m |I|^{s_o} = |I|^{s_o}.$$

As the open cover $\mathcal{J}$ was chosen arbitrarily, we have proved that for any open cover of Λ, $\mathcal{J}'$,

$$\sum_{J\in\mathcal{J}'} |J|^{s_o} \geq |I|^{s_o}.$$

This implies that

$$\mu_n^{*(s_o)}(\Lambda) \geq |I|^{s_o}. \tag{13}$$

From Equations (12) and (13), we have $\mu_n^{*(s_o)}(\Lambda) = |I|^{s_o}$. As $n \in \mathbb{N}$ was chosen arbitrarily, we have

$$\mu^{*(s_o)}(\Lambda) = \lim_{n\to\infty} \mu_n^{*(s_o)}(\Lambda) = |I|^{s_o}.$$

From Theorem 7, we see that the Hausdorff dimension of Λ is s_o. □

3.3. Nonplastic Impacts ($\varepsilon \neq 0$)

In this section we shall study the impacts that have very small coefficient of restitution, and in particular we will study the case with $\varepsilon = 0.01$. These impacts are essentially different from the plastic impacts as they are characterized by the knowledge of the 'position' and 'velocity' variables while plastic impacts are determined solely by the 'position' variable. Mathematically, plastic impacts are described by one dimensional systems while the nonplastic impacts are determined by two dimensional systems. We have already seen in Section 2 that under the condition $x(t) - z(t) > 0$ for all $t \in (t_k, t_{k+1})$, the two dimensional system describing the impact at time instant t_{k+1} is given by Equations (8) and (9). Using the dimensionless variables introduced in Section 2 and the nondimensionalized velocity variable $\gamma_k := v_k/\omega_n p$, we can rewrite these equations as

$$(1 + \nu \sin(\psi_k)) \cos(\eta \Delta_k^{\psi}) + \left(\varepsilon\gamma_k + \frac{\nu}{\eta}(1+\varepsilon)\cos(\psi_k)\right) \sin(\eta\Delta_k^{\psi}) - 1 - \nu\sin(\psi_{k+1}) = 0, \tag{14}$$

$$\gamma_{k+1} = (1 + \nu \sin(\psi_k)) \sin(\eta \Delta_k^{\psi}) - \left(\varepsilon\gamma_k + \frac{\nu}{\eta}(1+\varepsilon)\cos(\psi_k)\right) \cos(\eta\Delta_k^{\psi}). \tag{15}$$

We see that, given the characteristics of impact at instant t_k, the impact phase $\phi_k := \psi_k \bmod 2\pi$ and the dimensionless velocity γ_k; we can determine the characteristics $(\phi_{k+1}, \gamma_{k+1})$ of the next impact. We denote this map that takes the phase, ϕ, and velocity, γ, from one impact to the next by

$$F_{\eta,\nu,\varepsilon} : (\phi, \gamma) \to (\phi, \gamma).$$

We will show the existence of a two dimensional complex invariant set Λ_2 analogous to Λ in the one dimensional case, for a specific set of values, $(\eta, \nu, \varepsilon) = (0.2121, -0.2, 0.01)$. We consider the images of the rectangle $ABCD$ and $EFGH$ under the map $F_{\eta,\nu,\varepsilon}$ (see Figure 4), where

$$ABCD = \{(\phi, \gamma) : 1.11 < \phi < 1.15, -0.45 < \gamma < 0\},$$

$$EFGH = \{(\phi, \gamma) : 1.27 < \phi < 1.32, -0.45 < \gamma < 0\}.$$

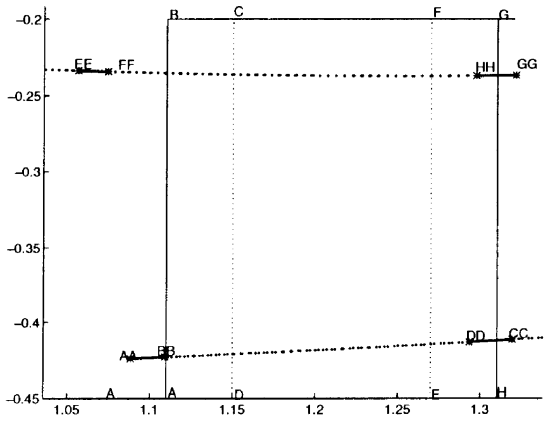

Figure 4. The topological horseshoe.

These images are shown in the same figure with emphasized points (e.g. AA) being the image of points (e.g. A). Note that the vertical distances are greatly contracted and the horizontal distances are expanded. We denote the vertical strips by $V_1 = ABCD$ and $V_2 = EFGH$ and their respective images (horizontal strips) by H_1 and H_2. We see that

$$F_{\eta,\nu,\varepsilon}(V_i) = H_i, \quad i = 1, 2$$

and thus we have a *topological horseshoe* [10]. For more detailed references on horseshoes, see [8] and [1]. Let $D = V_1 \cup V_2$. We define the invariant set Λ_2 by

$$\Lambda_2 = \bigcap_{n=-\infty}^{n=\infty} F_{\eta,\nu,\varepsilon}(D).$$

$F_{\eta,\nu,\varepsilon}$ having a horseshoe implies that Λ_2 contains [1, 8, 10]

1. countably many periodic orbits of arbitrarily high periods;
2. uncountably many nonperiodic orbits;
3. a dense orbit.

3.4. Analysis of the Mappings $f_{\eta,\nu}$ and $F_{\eta,\nu,\varepsilon}$

In previous sections, we have shown that for a specific set of parameters, $(\eta, \nu, \varepsilon) = (0.2121, -0.2, 0.0)$, the motion of the mass is complex on the invariant set $\Lambda \subset [1.11, 1.32]$ (in the plastic-impact case). We have seen that the trajectories of the mass are sensitive to initial conditions on this set. It is also possible to show that this set has zero Lebesgue measure. This means that there is a zero probability of 'typical' trajectories being in this set. In this section we shall investigate how this system behaves outside this set.

In Figure 5, we show the graph of $f_{\eta,\nu}$ over its full domain, i.e. $[0, 2\pi)$. We see that $(\partial f_{\eta,\nu}/\partial\phi)(\phi) = 0$ for all $\phi \in (3.38, 6.04)$. Impacts at these values are followed by a time interval in which the mass sticks on to the table. This happens when the force exerted on the mass by the spring is less than the force exerted on it by the table. This leads to a 2-periodic orbit (note that $\phi_2 = f_{\eta,\nu}(\phi_1)$ and $\phi_1 = f_{\eta,\nu}(\phi_2)$, and therefore, $\phi_i = f^2_{\eta,\nu}(\phi_i), i \in \{1, 2\}$ implying a 2-periodic orbit). We also see that all the orbits (that were simulated) eventually

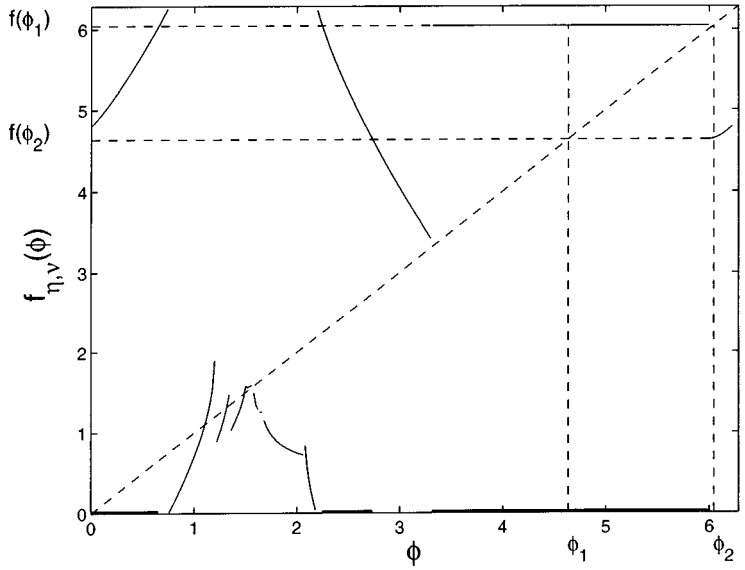

Figure 5. The graph of $f_{\eta,\nu}(\phi)$ for $\phi \in [0, 2\pi]$ is shown by the faint (curved) lines. $(\phi_1, \phi_2) = (4.64, 6.05)$ are on 2-periodic orbit. Simulation was done for $\phi \in [0, 2\pi]$ and $(\eta, \nu) = (0.2121, -0.2)$. $f_{\eta,\nu}(\phi) = \phi$ on the dashed line.

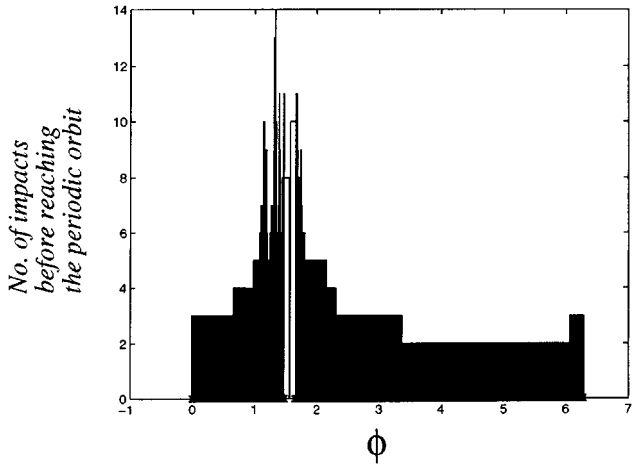

Figure 6. The histogram showing the number of impacts before reaching stable 2-periodic orbit of $f_{\eta,\nu}(\phi)$. Simulation was done for $\phi \in [0, 2\pi]$, $(\eta, \nu, \varepsilon) = (0.2121, -0.2, 0.0)$. Note that the number of impacts before reaching the 2-periodic orbit is very high near the invariant sets (in [1.1, 1.5]).

converge to this orbit. That is, this 2-periodic orbit attracts all the initial conditions chosen. The thickened part of the ϕ-axis shown in Figure 5 is a subset of the set of initial conditions that are attracted to the stable orbit. Note that, the proof of $f_{\eta,\nu}$ being sensitive to the initial conditions in the set [1.11, 1.32] depended only on the geometrical attributes of the graph of $f_{\eta,\nu}$ (i.e. the slope and the non invertibility), and we see the graph has the same properties in the set [1.32, 1.48]. This suggests the existence of another invariant set. So, although most of the initial conditions are attracted to the stable 2-periodic orbit, existence of these invariant sets shows that the dynamics of the mass in this model is complex. In Figure 6, we have

plotted histograms with the height of the bar denoting the number of impacts before which the trajectory reaches the periodic orbit. We observe that there is a relatively large transience (before settling to periodic orbits) corresponding to initial conditions near the invariant sets. This shows the effect of the invariant sets on the dynamics of the system.

Similar simulations were done in the nonplastic case for the same values of η and ν as in the one dimensional (plastic impact) case with different values of the coefficient of restitution ε. In these cases too, we observed that, there is a stable 2-periodic orbit which attracts all the initial conditions chosen. We saw that the trajectories took longer time to reach the periodic orbit with increase in values of coefficient of restitution. This fact can be utilized in order to predict the coefficient of restitution between the plate and the mass.

4. Single Impact Periodic Orbits

In the previous section we have analyzed the dynamics of the mass in the spring-mass system with specified values of the amplitude, ν, and frequency ratio, η. In this section we will study the dynamics of $f_{\eta,\nu}$ in the whole parameter space. We had mentioned earlier that it is difficult to get the evolution of impact phases as Equation (10) describing it is transcendental. However, we can analyze this equation for single-impact-periodic orbits. These orbits are said to occur if every impact occurs at the same phase (i.e. position) of the plate with the same velocity of the mass at every impact. In the plastic case, the motion of the mass after an impact is completely determined by the phase value at the impact, and hence impacts occurring with the same phase ensure single impact periodic orbits. An n-periodic single impact orbit is one in which the two consecutive nondimensionalized impact times (see Section 3) differ by $2\pi n$. Substituting this condition in Equation (10), we can show that the fixed point ϕ of the map is given by

$$(1 + \nu \sin(\phi)) \cos(2\pi n\eta) \; + \; \frac{\nu}{\eta} \cos(\phi) \sin(2\pi n\eta) - 1 - \nu \sin(\phi) = 0. \tag{16}$$

We define $\alpha := \eta(1 - \cos(2\pi n\eta))$, $\beta := \sin(2\pi n\eta)$ and $\theta := \tan^{-1}(\beta/\alpha)$. It can be seen that Equation (16) can be rewritten as

$$\sin(\phi - \theta) + \frac{\cos(\theta)}{\nu} = 0; \tag{17}$$

which gives explicit solution for ϕ. Note that all these calculations are valid under the assumption that the mass and the table separate just after the impacts and that 'sticking' does not occur. Now the stability of these fixed points can be determined by checking if the magnitude of the slope, $(\partial f_{\eta,\nu}/\partial\phi)(\phi)$, is less than unity. The slope is given by

$$\frac{\partial f_{\eta,\nu}}{\partial \phi}(\phi) = \frac{\frac{\nu}{\eta} \sin(\phi) \sin(2\pi n\eta) - \eta(1 + \nu \sin(\phi)) \sin(2\pi n\eta)}{-\eta(1 + \nu \sin(\phi)) \sin(2\pi n\eta) + \nu \cos(\phi) \cos(2\pi n\eta) - \nu \cos(\phi)}. \tag{18}$$

Figure 7a shows the various stable n-periodic fixed points as we vary η over the values $(0.01, 14)$ obtained by solving Equation (16). We see that slight changes in η lead to orbits of different periods. This shows that in this range of values of η, the motion of the mass is sensitive to the values of the frequency ratio, η.

Figure 7b shows how the n-periodic fixed points vary as we change ν over the values $(-0.9, 0.9)$ for a fixed $\eta = 0.237$ obtained by solving Equation (16). Again we observe that

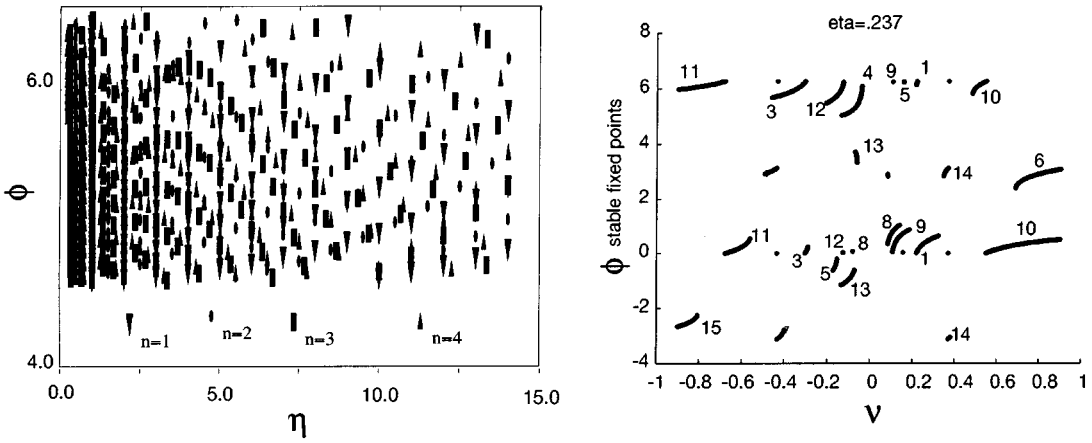

Figure 7. (a) The n-periodic fixed points with change in η with $\nu = 0.2$. (b) The n-periodic fixed points with change in ν with $\eta = 0.237$. The numbers on top of the curves denote the value of n.

slight changes in ν leads to fixed points of different periodic orbits. This implies that the motion of mass is sensitive to changes in the amplitude ratio (ν) of the system. Note that, in a n-periodic orbit, the table oscillates n times between consecutive impacts. Thus the impact frequency is a subharmonic of the frequency of the table.

5. Impact Oscillator with Soft Springs

In this section, we shall consider the equation

$$\ddot{x} + {\omega_n}^2 x = -g, \tag{19}$$

where g is the gravitational acceleration. The solution of this equation is given by

$$x(t) = \left(x_o + \frac{g}{w_n^2}\right)\cos(\omega_n(t - t_0)) + \frac{\dot{x}_o}{w_n}\sin(\omega_n(t - t_0)) - \frac{g}{\omega_n^2}, \tag{20}$$

$$\dot{x}(t) = \dot{x}_o \cos(\omega_n(t - t_0)) - \omega_n\left(x_o + \frac{g}{w_n^2}\right)\sin(\omega_n(t - t_0)). \tag{21}$$

Here, we will discuss the dynamics of the spring-mass system where the springs are soft. That is, we will study these equations as the natural frequency $\omega_n \to 0$. This is the reason, why we employ Equation (19) instead of Equation (1) as the origin in this coordinate system is independent of the natural frequency ω_n. The impact dynamics can be obtained (after carrying out computations as in Section 2) to get

$$(-p + \beta\sin(\omega t_k))\cos(\omega_n \Delta_k^t) + \frac{-\varepsilon v_k + (1+\varepsilon)\beta\omega\cos(\omega t_k)}{\omega_n}\sin(\omega_n \Delta_k^t)$$
$$- \frac{2g}{w_n^2}\sin^2\left(\frac{\omega_n}{2}\Delta_k^t\right) + p - \beta\sin(\omega t_{k+1}) = 0, \tag{22}$$

$$v_{k+1} = (-\varepsilon v_k + (1+\varepsilon)\beta\omega\cos(\omega t_k))\cos(\omega_n \Delta_k^t)$$
$$- \omega_n(-p + \beta\sin(\omega t_k))\sin(\omega_n \Delta_k^t) - \frac{g}{\omega_n}\sin(\omega_n \Delta_k^t). \tag{23}$$

We introduce a new variable $\psi := \omega t \bmod 2\pi$ with m such that $\omega t = \psi + 2\pi m$. In the new coordinates, Equations (22) and (23) become

$$\begin{aligned}
&(-p + \beta \sin(\psi_k)) \cos\left(\frac{\omega_n}{\omega}(\Delta_k^{\psi} + 2\pi\,\Delta_k^{m})\right) \\
&\quad + \frac{-\varepsilon v_k + (1+\varepsilon)\beta\omega\cos(\psi_k)}{\omega_n} \sin\left(\frac{\omega_n}{\omega}(\Delta_k^{\psi} + 2\pi\,\Delta_k^{m})\right) \\
&\quad - \frac{2g}{w_n^2} \sin^2\left(\frac{\omega_n}{2\omega}(\Delta_k^{\psi} + 2\pi\,\Delta_k^{m})\right) + p - \beta\sin(\psi_{k+1}) = 0, \qquad (24)
\end{aligned}$$

$$\begin{aligned}
v_{k+1} \;=\; &(-\varepsilon v_k + (1+\varepsilon)\beta\omega\cos(\psi_k)) \cos\left(\frac{\omega_n}{\omega}(\Delta_k^{\psi} + 2\pi\,\Delta_k^{m})\right) \\
&- \omega_n(-p + \beta\sin(\psi_k)) \sin\left(\frac{\omega_n}{\omega}(\Delta_k^{\psi} + 2\pi\,\Delta_k^{m})\right) \\
&- \frac{g}{\omega_n} \sin\left(\frac{\omega_n}{\omega}(\Delta_k^{\psi} + 2\pi\,\Delta_k^{m})\right). \qquad (25)
\end{aligned}$$

To find the fixed points ($\bar{\psi}$ and $\bar{v}$) of these equations, we use the relations $\psi_{k+1} = \psi_k = \bar{\psi}$, $\Delta_k^m =: m$ and $v_{k+1} = v_k = \bar{v}$ in Equations (24) and (25). Thus,

$$\begin{aligned}
&(-p + \beta\sin(\bar{\psi})) \cos\left(\frac{2\pi m\omega_n}{\omega}\right) + \frac{-\varepsilon\bar{v} + (1+\varepsilon)\beta\omega\cos(\bar{\psi})}{\omega_n} \sin\left(\frac{2\pi m\omega_n}{\omega}\right) \\
&\quad - \frac{2g}{w_n^2} \sin^2\left(\frac{2\pi m\omega_n}{\omega}\right) + p - \beta\sin(\bar{\psi}) = 0, \qquad (26)
\end{aligned}$$

$$\begin{aligned}
\bar{v} \;=\; &(-\varepsilon\bar{v} + (1+\varepsilon)\beta\omega\cos(\bar{\psi})) \cos\left(\frac{2\pi m\omega_n}{\omega}\right) \\
&- \omega_n(-p + \beta\sin(\bar{\psi})) \sin\left(\frac{2\pi m\omega_n}{\omega}\right) - \frac{g}{\omega_n} \sin\left(\frac{2\pi m\omega_n}{\omega}\right). \qquad (27)
\end{aligned}$$

These equations can be rewritten as

$$\begin{aligned}
&\underbrace{2(p - \beta\sin(\bar{\psi})) \sin^2\left(\frac{\pi m\omega_n}{\omega}\right) + \frac{\varepsilon(-p + \beta\sin(\bar{\psi})) \sin^2\left(\frac{2\pi m\omega_n}{\omega}\right)}{\omega_n\left(1 + \varepsilon\cos\left(\frac{2\pi m\omega_n}{\omega}\right)\right)}}_{A(\omega_n)} \\
&\quad + \underbrace{\frac{\varepsilon g \sin^2\left(\frac{2\pi m\omega_n}{\omega}\right)}{\omega_n^2\left(1 + \varepsilon\cos\left(\frac{2\pi m\omega_n}{\omega}\right)\right)}}_{B(\omega_n)} - \underbrace{\frac{2g}{\omega_n^2} \sin^2\left(\frac{\pi m\omega_n}{\omega}\right)}_{C(\omega_n)} + \underbrace{\frac{(1+\varepsilon)\beta\omega\cos(\bar{\psi}) \sin\left(\frac{2\pi m\omega_n}{\omega}\right)}{\omega_n\left(1 + \varepsilon\cos\left(\frac{2\pi m\omega_n}{\omega}\right)\right)}}_{D(\omega_n)}, \qquad (28)
\end{aligned}$$

$$\begin{aligned}
\bar{v} \;=\; &\underbrace{\frac{-\omega_n(-p + \beta\sin(\bar{\psi})) \sin\left(\frac{2\pi m\omega_n}{\omega}\right)}{1 + \varepsilon\cos\left(\frac{2\pi m\omega_n}{\omega}\right)}}_{E(\omega_n)} \\
&- \underbrace{\frac{g\sin\left(\frac{2\pi m\omega_n}{\omega}\right)}{\omega_n\left(1 + \varepsilon\cos\left(\frac{2\pi m\omega_n}{\omega}\right)\right)}}_{F(\omega_n)} + \underbrace{\frac{(1+\varepsilon)\beta\omega\cos(\bar{\psi})\cos\left(\frac{2\pi m\omega_n}{\omega}\right)}{1 + \varepsilon\cos\left(\frac{2\pi m\omega_n}{\omega}\right)}}_{G(\omega_n)}. \qquad (29)
\end{aligned}$$

Now,

$$\lim_{\omega_n \to 0} A(\omega_n) = 0, \quad \lim_{\omega_n \to 0} B(\omega_n) = \frac{\varepsilon g}{1+\varepsilon}\left(\frac{2\pi m}{\omega}\right)^2, \quad \lim_{\omega_n \to 0} C(\omega_n) = \frac{g}{2}\left(\frac{2\pi m}{\omega}\right)^2,$$

$$\lim_{\omega_n \to 0} D(\omega_n) = \frac{2\pi m}{\omega}\beta\omega\cos(\bar{\psi}), \quad \lim_{\omega_n \to 0} E(\omega_n) = 0, \quad \lim_{\omega_n \to 0} F(\omega_n) = \frac{2\pi mg}{\omega(1+\varepsilon)}$$

and

$$\lim_{\omega_n \to 0} G(\omega_n) = \beta\omega\cos(\bar{\psi}).$$

So, for every $\mu > 0$, there exists a $\delta > 0$ such that, for all $\omega_n < \delta$,

$$\frac{2\pi m}{\omega}\beta\omega\cos(\bar{\psi}) - \frac{g}{2}\left(\frac{2\pi m}{\omega}\right)^2 + \frac{\varepsilon g}{1+\varepsilon}\left(\frac{2\pi m}{\omega}\right)^2 + O(\mu) = 0$$

$$\Rightarrow \beta\omega\cos(\bar{\psi}) = \frac{(1-\varepsilon)\pi mg}{(1+\varepsilon)\omega} + O(\mu)$$

$$\Rightarrow \bar{\psi} = \cos^{-1}\left(\frac{(1-\varepsilon)\pi mg}{(1+\varepsilon)\omega^2\beta}\right) + O(\mu) = \left(\frac{1-\varepsilon}{1+\varepsilon}\right)\frac{2\pi m}{\rho} + O(\mu)$$

and

$$\bar{v} = \beta\omega\cos(\bar{\psi}) - \frac{2\pi mg}{\omega(1+\varepsilon)} + O(\mu) \Rightarrow \bar{v} = \frac{-\pi mg}{\omega} + O(\mu) \Rightarrow \bar{\lambda} = -2\pi m + O(\mu),$$

where $\rho = 2\omega^2\beta/g$, $\lambda := 2\omega v/g$ and a function $f(\mu)$ is said to be of $O(\mu)$ if there exists a constant K such that $0 \leq K < \infty$ and $\lim_{\mu \to 0} f(\mu) = K$. Note that the same results have been obtained in [1]. Also, in their model, an additional assumption [1, p. 103] that the distance that the *ball* travels under the influence of gravity is large compared with overall displacement of the table. From our analysis, we have shown that this assumption is unnecessary as no such assumption is made in our analysis. However, it is significant as it reduces the computational complexity of the problem by great amounts and so lends itself for easier understanding. The stability of these fixed points can be determined by checking if the eigenvalues of the Jacobian matrix,

$$J(\psi_k, \lambda_k) = \begin{bmatrix} \frac{\partial\psi_{k+1}}{\partial\psi_k} & \frac{\partial\psi_{k+1}}{\partial\lambda_k} \\ \frac{\partial\lambda_{k+1}}{\partial\psi_k} & \frac{\partial\lambda_{k+1}}{\partial\lambda_k} \end{bmatrix},$$

evaluated at these fixed points, lie inside the unit disk. This Jacobian matrix can be obtained from Equations (24) and (25) by taking the necessary partial derivatives. This matrix was evaluated at

$$\left(\psi_o := \cos^{-1}\left(\frac{1-\varepsilon}{1+\varepsilon}\right)\frac{2\pi m}{\rho}, \lambda_o := -2\pi m\right)$$

as $\omega_n \to 0$,

$$J(\psi_o, \lambda_o) = \begin{bmatrix} 1 - \frac{(1+\varepsilon)}{2}\alpha & -\frac{\varepsilon(1+\varepsilon)}{2} \\ \varepsilon\alpha & \varepsilon^2 \end{bmatrix},$$

where $\alpha = \sqrt{(1+\varepsilon)^2\rho^2 - (1-\varepsilon)^2(2\pi m)^2}$. We have already shown that the fixed points of the system can be made arbitrarily close to (ψ_o, λ_o) by taking sufficiently small values of ω_n. Therefore, the eigenvalues of the Jacobian evaluated at the fixed points can be made arbitrarily close to the eigenvalues of $J(\psi_o, \lambda_o)$. Thus we can learn about the fixed points of the system by studying the system at (ψ_o, λ_o). The stability of the fixed points is determined by the eigenvalues of this Jacobian matrix. The eigenvalues of this matrix are given by

$$\gamma_{1,2} = \frac{1}{2}\left(\left(1+\varepsilon^2 - \frac{1+\varepsilon}{2}\alpha\right) \pm \sqrt{\left(1-\varepsilon^2 - \frac{1+\varepsilon}{2}\alpha\right)^2 - 2\varepsilon^2(1+\varepsilon)\alpha}\right).$$

Note that the product of the eigenvalues is ε^2 independent of the value of ρ. Therefore, for nonplastic impacts (i.e. $0 < \varepsilon < 1$), either both these eigenvalues are inside the unit disk or one lies inside and the other lies outside the disk. This means that the fixed points are either sinks or saddles. Also we note that

$$\left(1-\varepsilon^2 - \frac{1+\varepsilon}{2}\alpha\right)^2 - 2\varepsilon^2(1+\varepsilon)\alpha = (1-\varepsilon^2)^2 + \left(\frac{1+\varepsilon}{2}\alpha\right)^2 + (1+\varepsilon)(1-\varepsilon^2)\alpha > 0,$$

and therefore the eigenvalues are real. We show that the fixed points are *saddles of the first kind* (i.e. $0 < \gamma_2 < 1 < \gamma_1$) if

$$\rho < 2\left(\frac{1-\varepsilon}{1+\varepsilon}\right)\sqrt{\pi^2 m^2 + 1},$$

saddles of the second kind (i.e. $\gamma_2 < -1 < \gamma_1 < 0$) if

$$\rho > \frac{1}{1+\varepsilon}\sqrt{\left(\frac{4(1-\varepsilon)}{1-2\varepsilon^2}\right)^2 + (1-\varepsilon)^2(2\pi m)^2}$$

and sinks for the remaining values of ρ. Orbits approaching and leaving the saddles of the latter kind do so in oscillatory manner and such fixed points are called *reflection hyperbolic*. The points

$$\rho_m := 2\left(\frac{1-\varepsilon}{1+\varepsilon}\right)\sqrt{\pi^2 m^2 + 1}, \quad \rho_m^f := \frac{1}{1+\varepsilon}\sqrt{\left(\frac{4(1-\varepsilon)}{1-2\varepsilon^2}\right)^2 + (1-\varepsilon)^2(2\pi m)^2}$$

are *bifurcation* values, at the first of which, a pair of fixed points appear in a saddle-node bifurcation and at the second of which a change of stability and a period doubling or flip bifurcation occurs. We can study if the mapping leads to period doubling by studying the derivatives of the reduced map obtained by using the center manifold theorem. However, we will analyze the one dimensional map in the plastic case (obtained by substituting $\varepsilon = 0$). The equation describing this system (as $\omega_n \to 0$) is given by

$$\rho\sin(\psi_k) + \rho\cos(\psi_k)(\Delta_k^{\psi} + 2\pi\Delta_k^m) - (\Delta_k^{\psi} + 2\pi\Delta_k^m)^2 - \rho\sin(\psi_{k+1}) = 0.$$

We define the map that takes ψ_k to ψ_{k+1} by $f : [0\ 2\pi] \to [0\ 2\pi]$, where ψ_k and $f(\psi_k)$ satisfy the above equation. By taking successive derivatives of this map, we note that

$$f(\psi_o, \rho_o) = 0, \quad \frac{\partial f}{\partial \psi}(\psi_o, \rho_o) = -1,$$

$$\frac{\partial f^2}{\partial \rho}(\psi_o, \rho_o) = 0, \quad \frac{\partial^2 f^2}{\partial \psi^2}(\psi_o, \rho_o) = 0,$$

$$\frac{\partial^2 f^2}{\partial \psi \partial \rho}(\psi_o, \rho_o) \neq 0, \quad \frac{\partial^3 f^2}{\partial \psi^3}(\psi_o, \rho_o) \neq 0,$$

where $\rho_o := \sqrt{(4 + (2\pi m)^2)}$. This implies that the map f undergoes a period doubling bifurcation [8, pp. 371–374].

6. Resonance Condition ($\omega_n/\omega = 1$)

In previous section, we dealt with the case in which the ratio between the natural frequency of the spring-mass system and the oscillation frequency of the table was very small (i.e. $\omega_n/\omega \to 0$). In this section, we shall study the case when these frequencies are the same (i.e. the resonance condition, $\omega_n/\omega = 1$). Here, equations describing the dynamics is obtained by substituting $\eta = 1$ in Equations (14) and (15). We obtain,

$$(1 + \nu \sin(\phi_k)) \cos(\Delta_k^\phi) + (\varepsilon\gamma_k + \nu(1+\varepsilon)\cos(\phi_k)) \sin(\Delta_k^\phi) - 1 - \nu \sin(\phi_{k+1}) = 0,$$

$$\gamma_{k+1} = (1 + \nu \sin(\phi_k)) \sin(\Delta_k^\phi) - (\varepsilon\gamma_k + \nu(1+\varepsilon)\cos(\phi_k)) \cos(\Delta_k^\phi),$$

These equations can be rewritten as

$$\alpha_k \sin(\theta_k + \Delta_k^\phi) = \alpha_{k+1} \sin(\theta_{k+1}) \tag{30}$$

$$\gamma_{k+1} = -\alpha_k \cos(\theta_k + \Delta_k^\phi), \tag{31}$$

where

$$\alpha_k = \sqrt{(1 + \nu \sin(\phi_k))^2 + (\varepsilon\gamma_k + \nu(1+\varepsilon)\cos(\phi_k))^2}$$

and

$$\tan(\theta_k) = \frac{1 + \nu \sin(\phi_k)}{(\varepsilon\gamma_k + \nu(1+\varepsilon)\cos(\phi_k)}.$$

6.1. Single Impact Periodic Orbits

For single impact periodic orbits, $\Delta_k^\phi = 0$ and $\Delta_k^\gamma = 0$, and therefore

$$\alpha_k \sin(\theta_k) = \alpha_{k+1} \sin(\theta_{k+1}) \Rightarrow \alpha_k \sin(\theta_k) = \text{ constant } = 1 + \nu \sin(\phi_o) := C_o$$

and

$$\gamma_k = -\alpha_k \cos(\theta_k + \Delta_k^\phi) \Rightarrow \gamma_k = -\nu \cos(\phi_o) =: \gamma_o,$$

where ϕ_o is the initial phase condition. Thus, in resonance condition, every initial phase value, ϕ_o can lead to a periodic orbit, if the velocity at the instant of impact is γ_o. The stability of these orbits can be found out by studying the Jacobian of this map at these values,

$$\lim_{\phi_{k+1} \to \phi_o} \frac{\partial F}{\partial(\phi_k, \gamma_k)}\bigg|_{\phi_o, \gamma_o} = \begin{bmatrix} 1 - \varepsilon\nu \sin(\phi_o) & -\varepsilon \\ \nu \sin(\phi_o)(1 - \varepsilon\nu \sin(\phi_o)) & -\varepsilon\nu \sin(\phi_o) \end{bmatrix}$$

and its eigenvalues are $\lambda_a := 0$ and $\lambda_b := 1-2\varepsilon\nu\sin(\phi_o)$. This implies that the periodic orbits are stable as long as $|\lambda_b| < 1$, i.e.

$$|1 - 2\varepsilon\nu\sin(\phi_o)| < 1.$$

6.2. Double Impact Periodic Orbits

Now let us study two impact periodic orbits. These orbits are said to occur if every second impact occurs at the same phase (i.e. position) of the plate and the same velocity. These orbits are characterized by $\phi_{k+2} = \phi_k$ and $\gamma_{k+2} = \gamma_k$. The first condition implies $\Delta_k^\phi = -\Delta_{k+1}^\phi$, $\alpha_{k+2} = \alpha_k$ and $\tan(\theta_{k+2}) = \tan(\theta_k)$. We shall use these relations to find the double impact periodic points. Note that $\tan(\theta_{k+2}) = \tan(\theta_k) \Rightarrow \sin(\theta_{k+2}) = \pm\sin(\theta_k)$.

Case 1. $\sin(\theta_{k+2}) = \sin(\theta_k)$.

$$\frac{\sin(\theta_k + \Delta_k^\phi)}{\sin(\theta_k)} = \frac{\sin(\theta_{k+1})}{\sin(\theta_{k+1} - \Delta_k^\phi)}$$

$$\Rightarrow \frac{\sin(\theta_k + \Delta_k^\phi) + \sin(\theta_k)}{\sin(\theta_k + \Delta_\phi^k) - \sin(\theta_k)} = \frac{\sin(\theta_{k+1}) + \sin(\theta_{k+1} - \Delta_k^\phi)}{\sin(\theta_{k+1}) - \sin(\theta_{k+1} - \Delta_k^\phi)}$$

$$\Rightarrow \frac{2\sin\left(\theta_k + \frac{\Delta_\phi^k}{2}\right)\cos\left(\frac{\Delta_k^\phi}{2}\right)}{2\sin\left(\frac{\Delta_\phi^k}{2}\right)\cos\left(\theta_k + \frac{\Delta_k^\phi}{2}\right)} = \frac{2\sin\left(\theta_{k+1} - \frac{\Delta_k^\phi}{2}\right)\cos\left(\frac{\Delta_k^\phi}{2}\right)}{2\sin\left(\frac{\Delta_k^\phi}{2}\right)\cos\left(\theta_{k+1} - \frac{\Delta_k^\phi}{2}\right)}$$

$$\Rightarrow \tan\left(\theta_k + \frac{\Delta_k^\phi}{2}\right) = \tan\left(\theta_{k+1} - \frac{\Delta_k^\phi}{2}\right)$$

$$\Rightarrow \theta_{k+1} = \theta_k + \Delta_k^\phi + n\pi, \quad n \in \mathbb{N} \Rightarrow \sin(\theta_{k+1}) = \pm\sin(\theta_k + \Delta_k^\phi).$$

Case 1.1. $\sin(\theta_{k+1}) = \sin(\theta_k + \Delta_k^\phi)$.
Using Equation (30), we deduce that $\alpha_{k+1} = \alpha_k$, which in turn implies that $\alpha_k = \alpha_o$ (a constant). Also, from these expressions and Equation (31), we have

$$\gamma_{k+2} = \gamma_k = -\alpha_{k+1}\cos(\theta_{k+1} - \Delta_k^\phi) = -\alpha_k\cos(\theta_k) \rightarrow \gamma_k = -\nu\cos(\phi_k).$$

This implies that the pair (ϕ_o, γ_o) are two impact periodic if $\gamma_o = -\nu\cos(\phi_o)$ and $(\partial\alpha_k/\partial\phi_k)(\phi_o, \gamma_o) = 0$. The last condition simplifies to (is equivalent to) $1 - \varepsilon\nu\sin(\phi_o) = 0$. Note that this condition can be rewritten as $1 - 2\varepsilon\nu\sin(\phi_o) = -1$ which the unstable one impact periodic orbit satisfied.

Case 1.2. $\sin(\theta_{k+1}) = -\sin(\theta_k + \Delta_k^\phi)$.
Using the fact that $\alpha_k >= 0$, $k \in \mathbb{N}$ and Equation (30) implies $\alpha_{k+1} = \alpha_k = 0$ or $\sin(\theta_{k+1}) = \sin(\theta_k + \Delta_k^\phi) = 0$.

Case 1.2.1. $\alpha_{k+1} = \alpha_k = 0$.
This implies the double impact periodic points are given by $(\phi_o = \sin^{-1}(-1/\nu), \gamma_o =$

$-(1+(1/e))\cos(\phi_o))$ and $(\phi_1 = \pi - \sin^{-1}(-1/\nu),\ \gamma_1 = -(1+(1/e))\cos(\phi_1))$.

Case 1.2.2. $\sin(\theta_{k+1}) = \sin(\theta_k + \Delta_k^{\phi}) = 0$.
These conditions imply that $\phi_1 = \sin^{-1}(-1/\nu)$, $\phi_o = \sin^{-1}(-1/\nu)$ (or vice-versa) and $\cos(\theta_{k+1}) = \pm 1$; and therefore, the following equations result

$$\gamma_o = s_o(\varepsilon\gamma_1 - (1+\varepsilon)\nu\cos(\phi_o)),$$

$$\gamma_1 = s_1(\varepsilon\gamma_o + (1+\varepsilon)\nu\cos(\phi_o)),$$

where $s_o, s_1 \in \{-1, 1\}$. On solving these, we obtain

$$\begin{pmatrix}\gamma_o\\ \gamma_1\end{pmatrix} = \begin{pmatrix}-1\\ 1\end{pmatrix}\nu\cos(\phi_o) \text{ or } \begin{pmatrix}\frac{1-\varepsilon^2}{1+\varepsilon^2}\\ \frac{(1+\varepsilon)^2}{1+\varepsilon^2}\end{pmatrix}\nu\cos(\phi_o) \text{ or}$$

$$\begin{pmatrix}-\frac{(1+\varepsilon)^2}{1+\varepsilon^2}\\ -\frac{1-\varepsilon^2}{1+\varepsilon^2}\end{pmatrix}\nu\cos(\phi_o) \text{ or } \begin{pmatrix}\frac{1+\varepsilon}{1-\varepsilon}\\ -\frac{1+\varepsilon}{1-\varepsilon}\end{pmatrix}\nu\cos(\phi_o),$$

where

$$\begin{pmatrix}\phi_o\\ \phi_1\end{pmatrix} = \begin{pmatrix}\sin^{-1}\left(\frac{-1}{\nu}\right)\\ \pi - \sin^{-1}\left(\frac{-1}{\nu}\right)\end{pmatrix} \text{ or } \begin{pmatrix}\pi - \sin^{-1}\left(\frac{-1}{\nu}\right)\\ \sin^{-1}\left(\frac{-1}{\nu}\right)\end{pmatrix}.$$

Case 2. $\sin(\theta_{k+2}) = -\sin(\theta_k)$.
This case does not lend itself to the kind of simplification that the previous case does. However, the double impact periodic orbits can be found by solving the corresponding equations numerically.

The stability of these periodic solutions can be found by studying the eigenvalues of the Jacobian matrix

$$\left.\frac{\partial F^2}{\partial(\phi,\gamma)}\right|_{\phi_o,\gamma_o} = \left.\frac{\partial F}{\partial(\phi,\gamma)}\right|_{\phi_1,\gamma_1}\left.\frac{\partial F}{\partial(\phi,\gamma)}\right|_{\phi_o,\gamma_o}.$$

$$\frac{\partial F}{\partial(\phi,\gamma)} = \begin{pmatrix}a_{11}(\phi,\gamma) & a_{12}(\phi,\gamma)\\ a_{21}(\phi,\gamma) & a_{22}(\phi,\gamma)\end{pmatrix},$$

where

$$a_{11}(\phi_o,\gamma_o) := 1 + \frac{\nu\cos(\phi_1) - \nu\cos(\phi_o)\cos(\phi_1-\phi_o) + \nu(1+\varepsilon)\sin(\phi_o)\sin(\phi_1-\phi_o)}{-(1+\nu\sin(\phi_o))\sin(\phi_1-\phi_o) + (\varepsilon\gamma + \nu(1+\varepsilon)\cos(\phi_o))\cos(\phi_1-\phi_o) - \nu\cos(\phi_1)},$$

$$a_{12}(\phi_o,\gamma_o) := \frac{-\varepsilon\sin(\phi_1-\phi_o)}{-(1+\nu\sin(\phi_o))\sin(\phi_1-\phi_o) + (\varepsilon\gamma + \nu(1+\varepsilon)\cos(\phi_o))\cos(\phi_1-\phi_o) - \nu\cos(\phi_1)},$$

$$a_{21}(\phi_o,\gamma_o) := (1+\nu\sin(\phi_o))\cos(\phi_1-\phi_o)(a_{11}-1) + \nu\cos(\phi_o)\sin(\phi_1-\phi_o)$$
$$+ (\varepsilon\gamma + \nu(1+\varepsilon)\cos(\phi_o))\sin(\phi_1-\phi_o)(a_{11}-1) - \nu(1+\varepsilon)\sin(\phi_o)\cos(\phi_1-\phi_o),$$

$$a_{22}(\phi_o,\gamma_o) := (1+\nu\sin(\phi_o))a_{12}\cos(\phi_1-\phi_o)$$
$$+ (\varepsilon\gamma + \nu(1+\varepsilon)\cos(\phi_o))\sin(\phi_1-\phi_o)a_{12} - \varepsilon\cos(\phi_1-\phi_o),$$

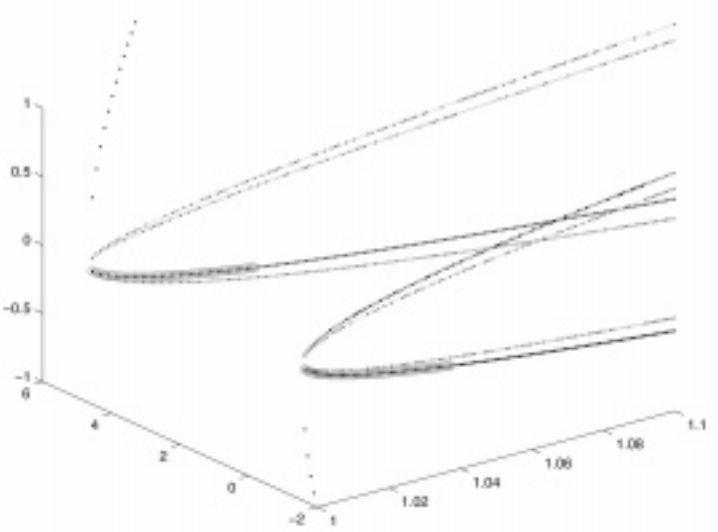

Figure 8. 2-impact periodic orbits. The circles (and the points within the circles) are the unstable double impact periodic orbits. The dotted curves correspond to fixed points that lead to 'sticking'.

where $(\phi_1, \gamma_1) = F(\phi_o, \gamma_o)$. All this analysis is true for those impact phases and velocities at which 'sticking' (described in Section 2 does not occur. The impact characterized by (ϕ_o, γ_o) is not 'sticking' if

$$(1 + \nu \sin(\phi_o)) \sin(\phi_1 - \phi_o) - (\varepsilon\gamma_o + (1 + \varepsilon)\nu \cos(\phi_o)) \cos(\phi_1 - \phi_o) + \nu \cos(\phi_o) < 0.$$

Figure 8 shows how these fixed points vary as the amplitude of vibration is increased. The circles (and the points within) are the unstable double impact periodic orbits while other dotted curves correspond to the fixed points which lead to 'sticking'.

7. Experimental Study

Since its inception, AFM has been employed in a wide range of applications. It uses a nano-sized tip in the end of a cantilever to sense the interaction between the tip and the sample (see Figure 9). Its tip displacement is measured by reflecting a laser beam off the back of the cantilever onto an array of photodiodes. The corresponding electrical signal gives a measure of the sample profile. Many techniques have been developed by modifying this idea for various applications of AFM in force measurements, magnetic spin detection and thermal measurements. In some of these techniques, the AFM tip, cantilever base or the sample are subjected to periodic oscillations [6, 11–13]. The experiment described below is one such case.

In previous sections, we showed the presence of complicated dynamics exhibited by the model we developed. In this section we will present experimental results which show the sensitivity of periodic orbits to the amplitude of vibration. The experimental setup is shown in Figure 9. The cantilever has a length of 45 μm, thickness of 2 μm (approx.) and width of 47 μm. An adequate model of the cantilever dynamics is

$$\ddot{y} + 2\xi\omega_o\dot{y} + \omega_o^2 y = f(t),$$

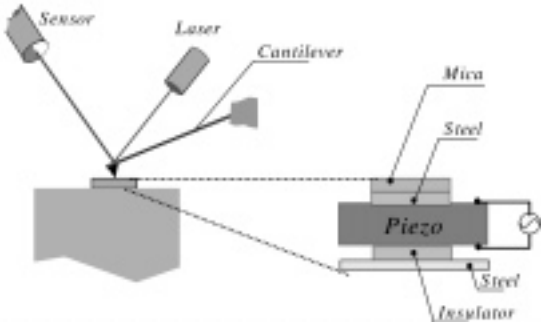

Figure 9. The experimental setup.

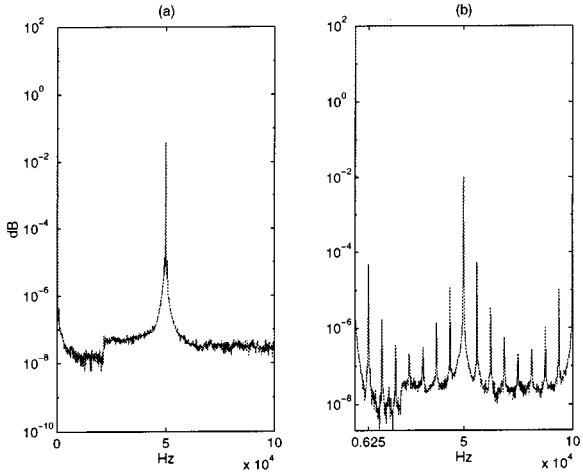

Figure 10. The sample is vibrated at the resonant frequency of the cantilever. The vertical axis reflects the displacement of the cantilever tip. In (a) the amplitude of vibration is lower and in (b) it is increased.

where ξ is the damping factor, ω_o is the natural frequency and $f(t)$ is the external force applied to the cantilever. The damping factor is due to surrounding air which can be neglected. Thus the cantilever motion is described by

$$\ddot{y} + \omega_o^2 y = f(t).$$

For the experiment, a steel puck was glued to the top of a piezo disc of thickness 1 mm (approx.) and diameter 10 mm. Mica wafer was attached to the steel puck. An insulator was glued to the bottom of the piezo disc which was firmly held to the base via another steel puck. Electrical leads were soldered to the top and bottom of the piezo which were connected to a signal source.

A sinusoidal voltage was applied to the piezo-disc at a frequency of 50 kHz (equal to the natural frequency of the cantilever). Figure 10 shows the effect of increasing the amplitude of vibration on the displacement of the cantilever. As can be seen there is eighth subharmonic appearing as the amplitude is increased. Further experiments to observe chaotic behavior are being conducted.

8. Conclusions

We have studied the dynamics of the mass in the mass-spring-vibrating table model (with plastic impacts) for a particular set of parameter values and have proved that there exist countably many periodic orbits, uncountably many nonperiodic orbits and a dense orbit in the invariant set, Λ. We proved that Λ is a Cantor set and computed its Hausdorff dimension. We considered the case in which impacts are not plastic (but with small coefficient of restitution) and showed the existence of another complex invariant set Λ_2 which implied complicated dynamics analogous to the one dimensional (plastic) case. We also showed existence of a stable 2-periodic orbit which attracted most of the initial conditions. This 2-periodic orbit persisted in the two dimensional (nonplastic) case. We found that these dynamics were sensitive to changes in the values of the frequency ratio, η, and the amplitude ratio, ν. The persistence of period doubling bifurcation in the bouncing ball model [1] to the case where mass with small spring constants was also presented. Similar studies were also done for the case when the forcing frequency (of the table) matched the natural frequency (of the mass-spring system).

Appendix

A.1. Algorithm for Computation of Next Impact Phase (ψ_{k+1}) from a Given Phase (ψ_k)

1. Choose a small $\delta > 0$.
2. Define $\alpha_n = \psi_k + n\delta$.
3. Define $s_n = sign((1 + \nu \sin(\psi_k)) \cos(n\eta\delta) + \frac{\nu}{\eta} \cos(\psi_k) \sin(n\eta\delta) - 1 - \nu \sin(\alpha_n))$.
4. Find the smallest positive number, n^*, such that $s_1 s_{n^*} = -1$.
5. Set $\psi_{k+1} = \alpha_{n^*}$.

This algorithm to solve Equation (10) can be explained as follows. We start from ψ_k and march incrementally (by δ) and calculate the sign of the left-hand side of Equation (10) (with ψ_{k+1} replaced by α_k) till it reverses. We know that the solution is between α_{n^*-1} and α_{n^*}. As δ is chosen small, we approximate the solution by α_{n^*}.

A.2. Some Definitions in Measure Theory

DEFINITION 1. Let X be any set and let $\mathcal{A}$ denote a nonempty family of subsets of X. We say $\mathcal{A}$ is an algebra of sets if it satisfies the following conditions:

1. $\phi \in \mathcal{A}$.
2. If $A \in \mathcal{A}$ and $B \in \mathcal{A}$ then $A \cup B \in \mathcal{A}$.
3. If $A \in \mathcal{A}$ then $X \setminus A \in \mathcal{A}$.

DEFINITION 2. Let X be any set and let $\mathcal{M}$ be a nonempty family of subsets of X. We say $\mathcal{M}$ is a σ-algebra of sets if

1. $\mathcal{M}$ is an algebra of sets.
2. $\mathcal{M}$ is closed under countable unions, i.e. if $\{A_k\} \subset \mathcal{M}$, then $\cup_{k=1}^{\infty} A_k \in \mathcal{M}$.

DEFINITION 3. Let $\mathcal{M}$ be a σ-algebra of subsets of X, and let μ be an extended real valued function on $\mathcal{M}$. We say that μ is a signed measure if $\mu(\phi) = 0$, and whenever $\{A_k\}$ is a sequence of pairwise disjoint elements of $\mathcal{M}$, then $\sum_{k=1}^{\infty} \mu(A_k)$ is defined as an extended real number with

$$\mu\left(\bigcup_{k=1}^{\infty} A_k\right) = \sum_{k=1}^{\infty} \mu(A_k).$$

If $\mu(A) \geq 0$ for all $A \in \mathcal{M}$, we say that μ is a measure. Also, the triple $(X, \mathcal{M}, \mu)$ is called a measure space. The members of $\mathcal{M}$ are called measurable sets.

DEFINITION 4. Let X be a set and let μ^* be an extended real valued function defined on subsets of X such that

1. $\mu^*(\phi) = 0$.
2. If $A \subset B \subset X$, then $\mu^*(A) \leq \mu^*(B)$.
3. If $\{A_k\}$ is a sequence of subsets of X, then

$$\mu^*\left(\bigcup_{k=1}^{\infty} A_k\right) \leq \sum_{k=1}^{\infty} \mu^*(A_k).$$

Then μ^* is called an outer measure on X.

DEFINITION 5. Let μ^* be an outer measure on X. A set $A \subset X$ is μ^*-measurable, if for all sets $E \subset X$,

$$\mu^*(E) = \mu^*(E \cap A) + \mu^*(E \setminus A).$$

THEOREM 5. *let X be a set, μ^* an outer measure on X, and $\mathcal{M}$ the class of μ^*-measurable sets. Then $\mathcal{M}$ is a σ-algebra and the set function μ defined on $\mathcal{M}$ by $\mu(A) = \mu^*(A)$ for all $A \in \mathcal{M}$ is a measure.*

Proof. See [9] for the proof. □

DEFINITION 6. Let X be a set and let $\mathcal{T}$ be a family of subsets of X such that the null set $\phi \in \mathcal{T}$. A function τ defined on $\mathcal{T}$ so that $\tau(\phi) = 0$ is called a premeasure, and we refer to the family $\mathcal{T}$ as a covering family for X.

THEOREM 6. *Let $\mathcal{T}$ be a covering family for a set X, and let $\tau : \mathcal{T} \to [0, \infty]$ with $\tau(\phi) = 0$. For $A \subset X$, let*

$$\mu^*(A) = \inf\left\{\sum_{k=1}^{\infty} \tau(T_k) : T_k \in \mathcal{T} \text{ and } A \subset \cup_{k=1}^{\infty} T_k\right\},$$

where an empty infimum is taken as ∞. Then μ^* is an outer measure on X.

Proof. See [9] for the proof. □

This way of obtaining outer measure is called *Method I construction of outer measure* and the corresponding measure (from Theorem 5) on X is called the measure obtained by *Method I*.

DEFINITION 7. Let X be a set and let $\rho : X \times X \to \mathbb{R}$. If ρ satisfies the following conditions, then we say ρ is a metric on X and call the pair (X, ρ) a metric space.

1. $\rho(x, y) \geq 0$ for all $x, y \in X$.
2. $\rho(x, y) = 0$ if and only if $x = y$.
3. $\rho(x, y) = \rho(y, x)$ for all $x, y \in X$.
4. $\rho(x, z) \leq \rho(x, y) + \rho(y, z)$ for all $x, y, z \in X$.

DEFINITION 8. Let $\mathcal{T}$ be a covering family on a metric space (X, ρ) with premeasure τ defined on it. For each $n \in \mathbb{N}$, let

$$\mathcal{T}_n = \left\{ T \in \mathcal{T} : \text{diameter}(T) \leq \frac{1}{n} \right\},$$

where $\text{diameter}(T) = \sup\{\rho(x, y) | x, y \in T\}$, then $\mathcal{T}_n$ is also a covering family for X for each $n \in \mathbb{N}$. For every $n \in \mathbb{N}$, we construct μ_n^* by Method I from $\mathcal{T}_n$ and τ. Since $\mathcal{T}_{n+1} \subset \mathcal{T}_n$,

$$\mu_{n+1}^*(E) \geq \mu_n^*(E)$$

for all $n \in \mathbb{N}$ and for each $E \subset X$. Thus the sequence $\{\mu_n^*(E)\}$ approaches a finite or infinite limit. We define μ_0^* as $\lim_{n\to\infty} \mu_n^*$ and refer to this as the outer measure determined by Method II from $\mathcal{T}$ and τ.

DEFINITION 9. Let X be a metric space, let $\mathcal{T}$ denote the family of all open subsets of X, and let $s > 0$. Let τ be a premeasure on $\mathcal{T}$ defined by

$$\tau(T) = (\text{diameter}(T))^s.$$

Then the measure $\mu^{*(s)}$ obtained from $\mathcal{T}$ and τ by Method II is called the Hausdorff s dimensional outer measure, and the resulting measure $\mu^{(s)}$, the Hausdorff s dimensional measure.

THEOREM 7. *If $\mu^{*(s)}(E) < \infty$ and $t > s$, then $\mu^{*(t)}(E) = 0$.*

Proof. See [9] for the proof. □

DEFINITION 10. Let E be a subset of metric space X, and let $\mu^{*(s)}(E)$ denote the Hausdorff s dimensional outer measure of E. If there is no value $s > 0$ for which $\mu^{*(s)}(E) = \infty$, then we let $\dim(E) = 0$. Otherwise, let

$$\dim(E) = \sup\{s : \mu^{*(s)}(E) = \infty\}.$$

Then $\dim(E)$ is called the Hausdorff dimension of E.

References

1. Guckenheimer, J. and Holmes, P., *Nonlinear Oscillations, Dynamical Systems and Bifurcation of Vector Fields*, Applied Mathematical Sciences, Vol. 42, Springer-Verlag, Berlin, 1993.
2. Shaw, S. W. and Holmes, P. J., 'A periodically forced impact oscillator with large dissipation', *Journal of Applied Mechanics* **50**, 1983, 849–857.

3. Hindmarsh, M. B. and Jefferies, D. J., 'On the motions of the offset impact oscillator', *Journal of Physics A: Mathematical and General* **17**, 1994, 1791–1803.
4. Nordmark, A. B., 'Non-periodic motion caused by grazing incidence in an impact oscillator', *Journal of Sound and Vibration* **55**(22), 1991, 279–297.
5. Chin, W., Ott, E., Nusse, H. E., and Grebogi, C., 'Grazing bifurcations in impact oscillator', *Physical Review E* **50**(6), 1994, 4427–4444.
6. Berg, J. and Briggs, G. A. D., 'Nonlinear dynamics of intermittent-contact mode atomic force microscopy', *Physical Review B* **55**(22), 1997, 14899–14908.
7. Ott, E., *Chaos in Dynamical Systems*, Cambridge University Press, Cambridge, 1994.
8. Wiggins, S., *Introduction to Applied Nonlinear Dynamical Systems and Chaos*, Texts in Applied Mathematics, Vol. 2, Springer-Verlag, Berlin, 1996.
9. Bruckner, A. M., Bruckner, J. B., and Thomson, B. S., *Real Analysis*, 1st edition, Prentice Hall, Englewood Cliffs, NJ 1997.
10. Moser, J., *Stable and Random Motions in Dynamical Systems*, Princeton University Press, Princeton, NJ, 1973.
11. Salapaka, S., Salapaka, M. V., Dahleh, M., and Mezic, I., 'Complex dynamics in repeated impact oscillators', in *Proceedings of 37th IEEE Conference on Decision and Control*, Tampa, FL, December, IEEE, New York, 1998, pp. 2053–2058.
12. Ashhab, M., Salapaka, M. V., Dahleh, M., and Mezic, I., 'Melnikov based dynamical analysis of microcantilevers in scanning probe microscopy', *Nonlinear Dynamics* **20**, 1999, 197–220.
13. M. Ashhab, M., Salapaka, M. V., Dahleh, M., and Mezic, I., 'Dynamical analysis of control of microcantilevers', *Automatica* **35**(10), 1999, 1663–1670.